Analyst

PAPER

View Article Online
View Journal | View Issue

Open Access Article. Published on 25 July 2016. Downloaded on 10/25/2025 11:51:01 PM.
This article is licensed under a Creative Commons Attribution-NonCommercial 3.0 Unported Licence.

Cite this: *Analyst*, 2016, **141**, 5784

A sandwich-like strategy for the label-free detection of oligonucleotides by surface plasmon fluorescence spectroscopy (SPFS)†

Qiang Su and Gilbert Nöll*

For the detection of oligonucleotides a sandwich-like detection strategy has been developed by which the background fluorescence is significantly lowered in comparison with surface-bound molecular beacons. Surface bound optical molecular beacons are DNA hairpin structures comprising a stem and a loop. The end of the stem is modified with a fluorophore and a thiol anchor for chemisorption on gold surfaces. In the closed state the fluorophore is in close proximity to the gold surface, and most of the fluorescence is quenched. After hybridization with a target the hairpin opens, the fluorophore and surface become separated, and the fluorescence drastically increases. Using this detection method the sensitivity is limited by the difference in the fluorescence intensity in the closed and open state. As the background fluorescence is mainly caused by non-quenched fluorophores, a strategy to reduce the background fluorescence is to cut the beacon in two halves. First a thiolated ssDNA capture probe strand (first half) is chemisorbed to a gold surface together with relatively short thiol spacers. Next the target is hybridized by one end to the surface-anchored capture probe and by the other to a fluorophore-labeled reporter probe DNA (second half). The signal readout is done by surface plasmon fluorescence spectroscopy (SPFS). Using this detection strategy the background fluorescence can be significantly lowered, and the detection limit is lowered by more than one order of magnitude. The detection of a target takes only a few minutes and the sensor chips can be used for multiple detection steps without a significant decrease in performance.

Received 16th May 2016,
Accepted 24th July 2016

DOI: 10.1039/c6an01129b

www.rsc.org/analyst

Introduction

In recent times there is a growing interest in the development of sensor platforms for the simple and fast detection of specific oligonucleotide sequences (DNA or RNA).[1–10] For the label-free detection of oligonucleotides in solution, different fluorescence based detection strategies applied in hybridization probes,[11,12] Taqman probes,[13,14] Scorpions,[15] or molecular beacons (MBs),[16] have been developed. Among the different probes MBs, which have been introduced by Tyagi and Kramer in 1996, are widely used.[17–19] MBs are DNA hairpin structures comprising a stem equipped with a fluorophore and a quencher in close proximity as well as a loop structure with a sequence complementary to that of the target. During hybridization with the target the hairpin opens, the fluorophore and the quencher get separated, and the fluorescence is switched on. While most MBs are applied in solution, there are also reports describing the use of molecular beacons at the solid–liquid interphase.[20–31] For this purpose the MBs were attached to a surface by different means. In the pioneering work of Miller, Krauss, *et al.* the molecular beacons were equipped with a thiol anchor (besides the chromophore) and adsorbed to a planar gold surface, which also served as the fluorescence quenching unit.[23,26–28,30] The corresponding fluorescence measurements were carried out by confocal fluorescence microscopy.[26,30] Following this approach, it was even possible to discriminate between a fully complementary single-stranded DNA (ssDNA) target and a target bearing a single base mismatch.[23,26–28,30] In 2011, Li *et al.* have used the same MB sequence as used previously by Miller, Krauss, *et al.*[26] for electric field assisted surface plasmon-coupled directional emission measurements (SPCE).[32] SPCE has been introduced in 2004 by Lakowicz as a new method of fluorescence detection, which can be seen as the inverse process of surface plasmon resonance (SPR) adsorption of thin metal films.[33] As an alternative to optical "signal on" sensors (detection of the fluorescence increase upon hybridization), the MB

Nöll Junior Research Group, Organic Chemistry, Chem. Biol. Dept., Faculty IV, Siegen University, Adolf-Reichwein-Str. 2, 57068 Siegen, Germany.
E-mail: noell@chemie.uni-siegen.de

† Electronic supplementary information (ESI) available: The optimization of the sensor chip preparation and performance, as well as further SPFS measurements. See DOI: 10.1039/c6an01129b

This journal is © The Royal Society of Chemistry 2016

Open Access Article. Published on 25 July 2016. Downloaded on 10/25/2025 11:51:01 PM.
This article is licensed under a Creative Commons Attribution-NonCommercial 3.0 Unported Licence.

concept has been adopted by Heeger, Plaxco, and coworkers for electrochemical sensors.[24,34–37] For this purpose the fluorophore has been replaced by a redox probe. After hybridization with the target the distance between the redox probe and gold electrode (*i.e.* the solid support) will change. Depending on the design of the MBs including the number of stem-loop structures, the distance between the redox probe and Au electrode may increase or decrease upon hybridization leading to a decrease[24,34] or increase[35,36] in the current for reduction and (re)oxidation of the redox probe ("signal off" or "signal on" sensors). Seminal work towards understanding and improving the performance of electrochemical DNA sensors and developing new sensing architectures has been carried out in the groups of Heeger, Plaxco, and Ricci.[2,5,38–40] In our previous work we have used surface plasmon fluorescence spectroscopy (SPFS)[4,41–43] as a better and faster readout technique than fluorescence microscopy for optical "signal on" sensors.[44] For sensor chip preparation fluorophore (Cy5) labeled MBs equipped with three dithiane anchors were coadsorbed with short thiols serving as spacers on a gold-coated glass slide. The working principle of this MB-SPFS sensor is shown in Scheme 1. Rather close to the surface the fluorescence is quenched by energy transfer to the gold surface (the MB is in the closed state). Upon hybridization with the target the distance between the gold surface and fluorophore increases, and the fluorophore can be excited by the enhanced evanescent field caused by the surface plasmons. On the other hand, the intensity of the evanescent field decays exponentially with distance. Hence, there is an optimum distance for fluorescence detection for the MB in the open state, at which strong excitation without significant quenching can be achieved. For maximum fluorescence intensity an optimum distance of about 20 nm orthogonal to the surface has been estimated (the exact value depends also on the physical properties of the applied fluorophore).[41]

During our work we have studied the same beacon sequence as Miller, Krauss *et al.* in their pioneering research on surface bound MBs,[26] and additionally we have studied a new significantly longer sequence for which we pointed out the differences.[44] We optimized the surface chemistry (*i.e.* the conditions for self-assembly, the choice of the thiol spacer, and the thiol anchor of the MB) leading to homogeneous sensor surfaces. Our SPFS-MB sensors comprise a low detection limit (down to 500 pM), a fast response time (5–20 min), and they can be reused several times. We even observe a linear behavior between the fluorescence increase and target concentration when the hybridization is carried out only for five minutes.[44]

To further decrease the detection limit of our SPFS-MB sensors we need to increase the difference in fluorescence intensity between the open and the closed state of the MBs, *i.e.* to minimize the fluorescence signal in the closed state and/or to maximize the fluorescence after hybridization with the target. A strategy to maximize the fluorescence in the open state is to optimize the length and orientation of the fluorophore with respect to the surface after hybridization with the target. A distance has to be reached at which quenching is avoided and strong fluorescence excitation is possible. In this contribution we focus on minimizing the fluorescence intensity in the closed state (the background fluorescence), which is (disregarding instrumental parameters) mainly caused by fluorophores close to the surface, which are not completely quenched. The most efficient way to diminish this fluorescence is to remove the fluorophore. This can be literally done quite easily by cutting the beacon into two pieces. As shown in Scheme 2 this will result in a sandwich-like detection procedure.[10,45–48]

First the surface has to be modified with the thiol-anchored part of the MB serving as a capture probe. Next the target is hybridized to the capture probe before finally the fluorophore-modified reporter probe is hybridized. Following this sandwich-like procedure theoretically the target will be detected only if it is complementary to capture and reporter probes. Furthermore, there will be no fluorescence originating from the fluorophore, since the fluorophore can bind only to the surface, if the target is present (assuming there is no unspecific binding). However, if this procedure is carried out using exactly the same sequence and number of bases as previously for the intact MB for comparison, serious problems will arise. The separated capture probe and reporter probe sequences may be too short for efficient hybridization with the target at room temperature. In addition even in the absence of the target a false positive signal may be obtained if the stem region of the capture probe and reporter probe hybridize (even though the intensity of this signal is expected to be low since

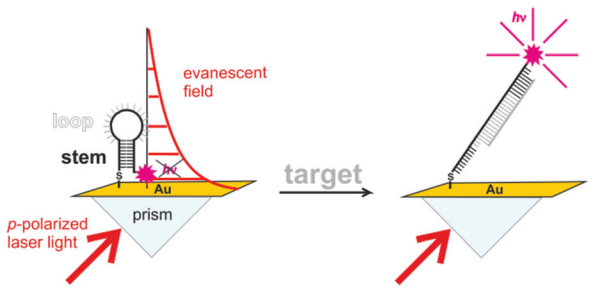

Scheme 1 Working principle of the MB-SPFS sensor as described in ref. 44.

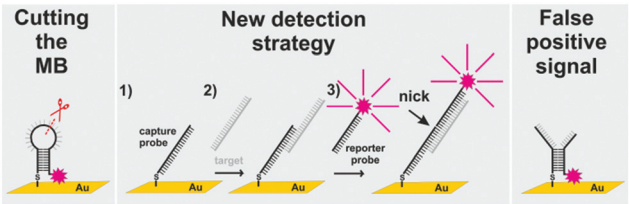

Scheme 2 By cutting the MB into two pieces a sandwich-like detection strategy arises. Following this strategy a nick remains in the final dsDNA structure, which is absent in the initial MB structure after hybridization with target. Furthermore, a false positive signal may be detected by this strategy as shown on the right.

Open Access Article. Published on 25 July 2016. Downloaded on 10/25/2025 11:51:01 PM.
This article is licensed under a Creative Commons Attribution-NonCommercial 3.0 Unported Licence.

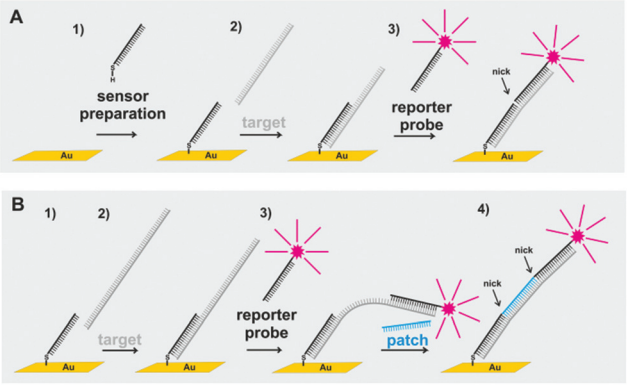

Scheme 3 Detection strategies applied in this work. (A) (1) The sensor chip is modified with a capture probe of 20 bases. This is followed by the adsorption of a mixture of mercaptobutanol and mercaptopropionic acid (MCB/MPA, 1 : 1) to remove non-specifically adsorbed ssDNA (for clarity not shown). (2) A target of 40 bases is captured. (3) A fluorophore-comprising reporter probe is hybridized, readout by SPFS is possible. (B) (1) The sensor chip is modified with a capture probe of 20 bases as before. (2) A target of 60 bases is captured. (3) A fluorophore-comprising reporter probe is hybridized at the upper end of the target, readout by SPFS is possible. (4) The dsDNA/ssDNA/dsDNA assembly is stiffened by a patch of 20 bases.

the fluorophore is located close to the surface). Furthermore after the target and reporter probe are bound to the capture probe a nick will remain in the MB as shown in Scheme 2, by which additional flexibility will be introduced.

Therefore the distance between the fluorophore and surface may be different than for the intact MB. For these reasons we refrained from using the same sequence and number of bases as previously for the MB comprising 36 bases with a detection limit of 500 pM.[44] Instead we used a capture probe of 20 bases, a reporter probe of 20 bases, and a target of 40 bases as outlined in Scheme 3A. The same capture probe and reporter probe comprising 20 bases each can also be employed to trace a target comprising 60 bases as shown in Scheme 3B. After hybridization of the capture probe and reporter probe with the target at the outer ends, a flexible internal region of 20 bases remains at the target. This internal region can be later stiffened by hybridization with a patch, *i.e.* complementary ssDNA of 20 bases. As it was our interest to study the general effects of the structural properties of DNA assemblies on the molecular scale we did not choose a sequence belonging to a specific genetic disease or disorder. Instead sequences were chosen, which allowed unambiguous hybridization.

Experimental section

Chemicals

Chemicals for buffer preparation (NaCl, Tris, $MgCl_2$, NaH_2PO_4) were purchased from Roth Chemicals. The thiols 4-mercapto-1-butanol (MCB), 6-mercaptohexanol (MCH), 11-mercapto-1-undecyl dihydrogen phosphate (MDPA), and 3-mercapto-1-propanesulfonic acid sodium salt (MPS) were purchased from Sigma-Aldrich Chemie GmbH, (Steinheim, Germany), and 3-mercaptopropionic acid (MPA) was purchased from Alfa Aesar GmbH & Co. KG (Karlsruhe, Germany). These compounds were used as received without further purification.

All oligomers were purchased from Eurogentec S.A. Liège Science Park, (Seraing Belgium) or from Metabion GmbH, (Martinsried Germany). For SPFS measurements a ssDNA capture probe (CP) comprising 20 bases (5′-AAC TAC TGG GCC ATC GTG AC-3′) modified at the 5′-end with three dithiane groups[49,50] introduced by the use of dithiol-phosphoramidite (6750.6 g mol^{-1}), as well as the ssDNA reporter probe (RP) with 20 bases (5′-TGA GGT GAA AGT GTG AGT GC-3′) modified with a Cy 5® at the 3′-end (7115.2 g mol^{-1}) were used. Two types of targets with different lengths, 40 bases (5′-GCA CTC ACA CTT TCA CCT CA G TCA CGA TGG CCC AGT AGT T-3′) with 12151.9 g mol^{-1} and 60 bases (5′-GCA CTC ACA CTT TCA CCT CA GCA TCA GTC TCT CGT ACA GT GT CAC GAT GGC CCA GTA GTT-3′) with 18281.9 g mol^{-1} were analyzed, respectively. For patching studies, the patch containing 20 bases (5′-ACT GTA CGA GAG ACT GAT GC-3′) with 6166.1 g mol^{-1} can be hybridized with the centered sequence of the 60 bases target.

Preparation of the gold substrates

SPR-chip preparation: gold substrates were prepared by vacuum evaporation of gold (48 nm layer thickness) onto cleaned glass slides (n_{BK7} = 1.515 at 633 nm), which were pre-coated with a thin titanium layer (1.5 nm) to improve adhesion. The gold substrates were freshly cleaned prior to use by treatment with a piranha solution (3 : 1 concentrated H_2SO_4/30%H_2O_2, CAUTION: piranha solution reacts violently with most organic materials and must be handled with extreme care) for 5 min at room temperature and then rinsed with pure water.

SPR and SPFS

For SPR and SPFS a commercially available setup from Res-Tec (Resonant Technologies, Framersheim, Germany) was used.

Immobilization procedure

The thiolated ssDNA was adsorbed on the SPR chip in the following way. The capture probe DNA was dissolved in Tris buffer and adsorbed to the gold surface for 1 h. The thiolated ssDNA (modified with three 1,2-dithiane rings) was used at a concentration of 5 μM. After adsorption was completed, the surface was rinsed with buffer and MQ water. To replace non-specifically adsorbed DNA strands and saturate free sites at the gold surface, in the next step a mixture of low-molecular weight thiols was adsorbed.[51] Equimolar amounts of mercaptobutanol (MCB) and mercaptopropionic acid (MPA), dissolved in water at a 1 mM overall concentration, were adsorbed on the DNA–gold surface for 30 min followed by rinsing with MQ water. Besides these thiols, other thiols were investigated as spacers as well. Each step of surface modification was monitored by SPR.

 This journal is © The Royal Society of Chemistry 2016

Open Access Article. Published on 25 July 2016. Downloaded on 10/25/2025 11:51:01 PM.
This article is licensed under a Creative Commons Attribution-NonCommercial 3.0 Unported Licence.

Calculation of the surface coverage of the capture probe

From the shift in the SPR angular scan curves measured before and after preparation of the capture probe layer, the surface coverage of the capture probe was calculated as already described before.[44,52] By fitting the angular scan curves measured before and after layer formation to a Fresnel algorithm assuming a refractive index n_A of 1.5 for DNA,[53] the thickness d_A of the individual DNA layers can be obtained. For this purpose the software WinSpall (version 3.0.2.0, Max Planck Institute of Polymer Research, Mainz, Germany) was used. Furthermore, the mass of the DNA films after adsorption of the capture probe can be calculated using Feijter's equation.[54]

$$M = d_A \frac{n_A - n_{sol}}{dn/dc}$$

In Feijter's equation d_A is the thickness of the layer, and n_A and n_{sol} are the refractive indices of the layer and buffer, respectively.[54] The quotient dn/dc is the refractive index increment of the adsorbed layer.[54] Assuming a value of dn/dc = 0.175 $cm^3\ g^{-1}$ for DNA,[55] n_A = 1.5, and n_{sol} = 1.33, a value of M (ng cm^{-2}) was obtained for the capture-probe layer. In order to calculate the surface coverage in mol cm^{-2}, the values obtained for M in ng cm^{-2} were divided by the molecular weight (6750.6 g mol^{-1}) of the capture probe with three dithianes. The molecular weight of the capture probe with three dithianes is much larger than that of MCB/MPA (6750.6 g $mol^{-1} \gg 106$ g mol^{-1}). Therefore the contribution of the MCB/MPA spacers was neglected at ratios between the capture probe and MCB/MPA of (5 : 0), (5 : 10), (5 : 50), and (5 : 125). However, for the capture probe surfaces prepared by co-adsorption of the capture probe and thiol spacers at an overall ratio of 5 : 250 the surface coverage of the capture probe was rather low, and the signal contribution from MCB/MPA could not be neglected anymore during the calculation of the surface coverage. Therefore in a control experiment SPR sensor chips were modified with MCB/MPA only, following the same procedure (not shown). To determine the surface coverage of the capture probe DNA, the surface bound mass calculated for the control experiment was subtracted from the surface bound mass calculated for the sensor chips modified with capture probe DNA and MCB/MPA.

Results and discussion

Optimization of the sensor performance

As first measurements showed that the new detection strategy is working, we used the three component detection strategy outlined in the steps 1–3 in Scheme 3A with the target comprising 40 bases ($\mathbf{T_{40}}$) in order to optimize the experimental conditions with respect to the salt composition of the buffer solution (it is known that the presence of mono- and bivalent cations has a strong influence on the DNA hybridization efficiency[56]) and the procedure for the preparation of the sensor chip. As a capture probe we used the $(1,2\text{-dithiane})_3$ modified ssDNA, since by the use of six sulfur–gold (or sulfur–silver) bonds a highly stable functionalization of metal surfaces can be obtained.[57,58] To keep the experiments straightforward, the reporter probe and the target were first hybridized in solution before they were added to the capture probe-modified surface rather than carrying out the steps 2 and 3 of Scheme 3 stepwise. For this purpose 100 μL of target solution (at different target concentrations) were first mixed with 100 μL of a 100 nM solution of the reporter probe at a concentration of 100 nM for five minutes and then incubated. As in our previous studies of surface bound MBs,[44] for all experiments 2 mM Tris-buffer at pH 7.5 was used as standard buffer. As shown in Fig. S1A and S1B in the ESI,† the NaCl and the $MgCl_2$ concentrations were varied. The best performance, *i.e.* the largest fluorescence increase during the detection event was obtained at a NaCl concentration of 200 mM and an $MgCl_2$ concentration of 6 mM. Using this salt concentration, in Tris buffer a larger increase in fluorescence during the detection of $\mathbf{T_{40}}$ than in phosphate buffer could be obtained (shown in Fig. S1C†). Therefore 2 mM Tris-buffer at pH 7.5 containing 200 mM NaCl and 6 mM $MgCl_2$ was used for all further measurements. Next different sensor chips prepared by co-adsorption of the capture probe at a concentration of 5 μM and equimolar mixtures of MCB/MPA at different concentrations were compared. To complete the sensor chip preparation the adsorption of the capture probe was followed by incubation with a mixture of MCB/MPA (0.5 mM each) in pure water for 30 min before the surface was rinsed with buffer. From the shift in the SPR angular scan curves measured before and after preparation of the capture probe layer the surface coverage of the capture probe was calculated as described elsewhere.[44] For surfaces prepared with a ratio between the capture probe and MCB/MPA of 5 : 0, 5 : 10, 5 : 50, 5 : 125, and 5 : 250 surface coverages of 1.6×10^{-11} mol cm^{-2} (d_A = 1.1 nm), 1.5×10^{-11} mol cm^{-2} (1.0 nm), 1.3×10^{-11} mol cm^{-2} (0.9 nm), 0.7×10^{-11} mol cm^{-2} (0.5 nm), and 0.4×10^{-11} mol cm^{-2} (0.3 nm) were calculated, respectively from the obtained values for the surface thickness given in brackets.

As shown in Fig. 1 the best performance was obtained at the highest surface coverage of the capture probe. For this purpose the capture probe had to be adsorbed in buffer in the absence of MCB/MPA for 1 h before a mixture of MCB/MPA 0.5 mM each in pure water was incubated for 30 min followed by rinsing the surface with buffer. This resulted in a surface coverage of 1.6×10^{-11} mol cm^{-2}. From this surface coverage a center to center distance of 3.2 nm between two adjacent ssDNA capture probe strands can be calculated as shown in the ESI† (during this calculation the geometrical surface area was used and any effects of surface roughness were neglected). Besides, a mixture of MCB/MPA longer thiol spacers such as MCH and MDPA, and MPS were evaluated as well. As shown in Fig. S2 in the ESI† the best performance was obtained with the mixture of MCB and MPA, possibly because the short thiols do not sterically hinder the hybridization of the target at the surface.

Open Access Article. Published on 25 July 2016. Downloaded on 10/25/2025 11:51:01 PM.
This article is licensed under a Creative Commons Attribution-NonCommercial 3.0 Unported Licence.

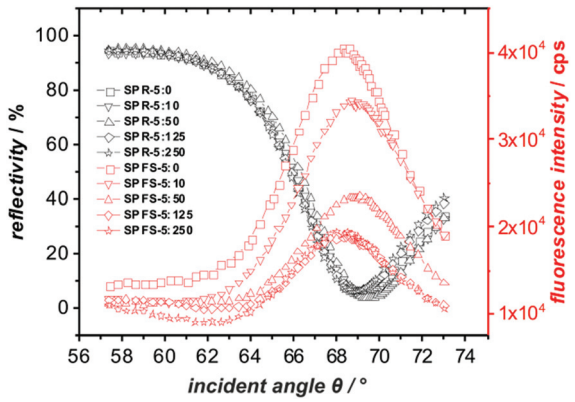

Fig. 1 SPR (black) and SPFS (red) angular scan curves measured at surfaces prepared by chemisorption of the capture probe at a concentration of 5 μM mixed with different concentrations of equimolar MCB/MPA (the total concentration of thiol spacers was 0 μM, squares; 10 μM, down triangles; 50 μM, up triangles; 125 μM, diamonds; 250 μM, stars). Thereafter a mixture of 1 mM MCB/MPA (each 0.5 mM) in water was incubated for 1 h before the surface was rinsed with buffer. Subsequently 5 nM T_{40} mixed with 50 nM reporter probe was incubated for 10 min, followed by rinsing with buffer for 5 min, before the angular scan curves were collected.

Determination of the detection limits for the targets comprising 40 and 60 bases, T_{40} and T_{60}

During the optimization of the sensor performance the reporter probe and the target were first hybridized for 5 min in solution before they were added to the capture probe-modified surface. The detection limit was determined by this procedure as shown in Fig. 2, and also by carrying out the steps 2 and 3 of Scheme 3 stepwise as shown in Fig. S3 of the ESI.† For both procedures a detection limit of 50 pM was determined. The resulting architecture at the surface of the sensor chip comprises a Cy5-labelled surface grafted dsDNA structure with an overall length of 40 base pairs (bp). The resulting detection limit is 10–20 times lower than the detection limit determined previously for MBs with 36 and 38 bases.[44] By following the new detection strategy outlined in Scheme 3A the background fluorescence could be lowered from around 1.5×10^5 photomultiplier counts per second (cps) obtained for the MBs in the closed state[44] to around 6.5×10^3 as shown in Fig. 2 and S3.† Also for the detection of the longer target comprising 60 bases $\mathbf{T_{60}}$, the two different detection procedures, *i.e.* pre-hybridization of the target and reporter probe *vs.* stepwise hybridization at the surface as outlined in the steps 1–4 of Scheme 3B, were compared. Also for the longer target $\mathbf{T_{60}}$ a detection limit of 50 pM was obtained for both procedures as shown in Fig. S4 and S5 of the ESI.† Apparently the increase in the target length from 40 to 60 bases has no strong influence on the fluorescence intensity and on the detection limit. A detailed comparison of the detection of the targets $\mathbf{T_{40}}$ and $\mathbf{T_{60}}$ at the same sensor chip follows in the next section. It is worth noting that for the concentration dependent measurements shown in Fig. 2

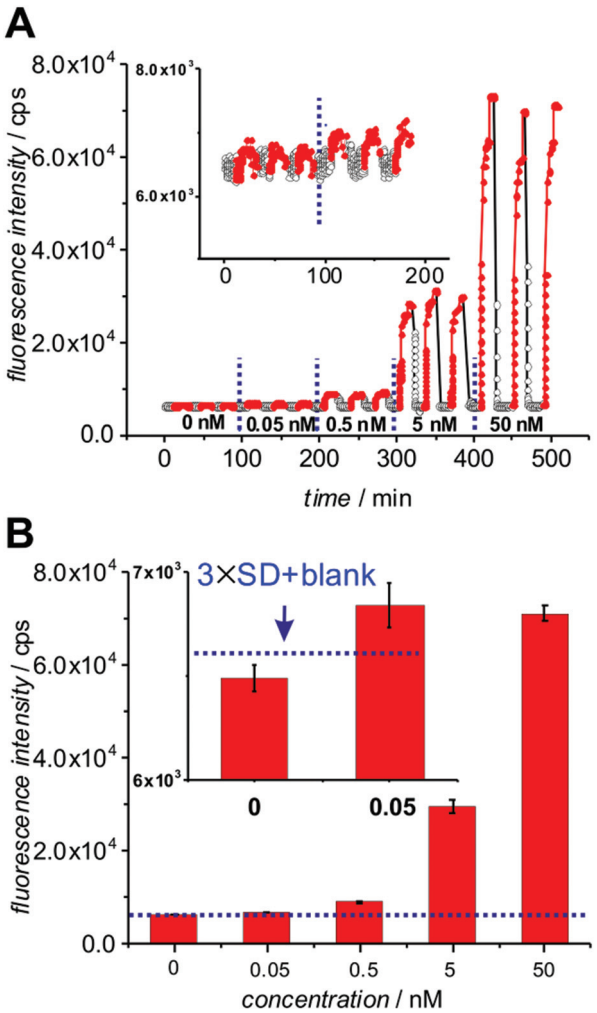

Fig. 2 Determination of the detection limit for the 40 bases target (T_{40}). For signal readout 100 μL target solution (at different target concentrations) were first mixed with 100 μL of a 100 nM solution of the reporter probe and then incubated. (A) SPFS kinetic scan curves measured at a fixed angle of 68.8° for target concentrations from 0 nM to 50 nM. The fluorescence signal (red) is shown for several detection events carried out at the same chip. In between the individual detection events the sensor surface was regenerated by rinsing with pure water followed by equilibration with buffer until a stable fluorescence background was reached (black). (B) Average fluorescence signal of three measurements on the same sensor chip detected after 10 min incubation with the mixtures and subsequent rinsing with buffer. The threshold (dashed line) is equal to the sum of the blank and three times of standard deviation (SD). The blank is the average value of negative control (0 nM target). The error bars show the confidence interval for $P = 0.95$.

a final reporter probe concentration of 50 nM was used, and therefore the maximum target concentration studied systematically was 50 nM. In an additional experiment the target and reporter probe concentrations were both increased to 500 nM. In that case the fluorescence increase was so strong (≥2.8 × 10 cps) that the shutter in front of the photomultiplier closed in order to prevent the photomultiplier from being damaged.

 This journal is © The Royal Society of Chemistry 2016

Open Access Article. Published on 25 July 2016. Downloaded on 10/25/2025 11:51:01 PM.
This article is licensed under a Creative Commons Attribution-NonCommercial 3.0 Unported Licence.

Comparison of the detection of the targets T_{40} and T_{60} at the same sensor chip

In order to compare the detection of the targets $\mathbf{T_{40}}$ and $\mathbf{T_{60}}$ at the same sensor chip both targets were detected at a concentration of 5 nM as shown in Fig. 3. To limit the number of involved steps, the target was hybridized with the reporter probe prior to incubation at the sensor surface. After detection of the targets $\mathbf{T_{40}}$ and $\mathbf{T_{60}}$ the sensor surface was regenerated by rinsing with pure water (resulting in complete dehybridization of the target) followed by equilibration in buffer solution.

As can be seen from Fig. 3, when the surface is rinsed with buffer solution after incubation with the forty bases target $\mathbf{T_{40}}$ hybridized with the reporter probe for 5 min, there was a slight further increase of the fluorescence signal, which might be explained by the hybridization of further target molecules due to convection. When rinsing with buffer was continued for a few minutes the fluorescence signal became constant. We explain the rather large increase in fluorescence after incubation with the target hybridized with the reporter probe by the assumption that the resulting dsDNA hybrid comprising 40 bp with a length of about 14 nm is standing more or less upright at the surface (at a certain angle). Furthermore, the capture probe molecules are grafted to the surface at high density resulting in electrostatic repulsion between individual capture probe strands, and between target strands and the target containing the dsDNA structure. Therefore the Cy5 labeled dsDNA assembly is expected to be pushed away from the surface and oriented towards the solution. As a consequence the Cy5 dye is located at a distance at which the quenching by energy transfer to the gold surface is already relatively low, and the fluorescence can be strongly excited by the evanescent field. When the larger target $\mathbf{T_{60}}$ was incubated after hybridization with the reporter probe the increase in the fluorescence signal was initially quite low as shown in Fig. 3. Even though the surface grafted dsDNA substructure of 20 bp is expected to be oriented away from the surface pointing towards the solution, the centered 20 unpaired bases of the target comprise a highly flexible region, which allows the outer dsDNA substructure of 20 bp bearing the Cy5 label to approach the surface rather close. Therefore the majority of the fluorescence signal is quenched. The situation changes during incubation with the patch. By hybridization of the patch with the centered flexible region of the target a rather stiff dsDNA assembly of 60 bp with an overall length of about 20 nm is formed, which is more or less standing at the surface increasing the distance between the fluorophore and surface and thereby causing a large increase in the fluorescence signal. The fact that the fluorescence signal becomes even stronger than for the detection of the forty bases target $\mathbf{T_{40}}$ implies that for the target $\mathbf{T_{60}}$ the Cy5 dye is located further away from the surface and thus less of the fluorescence is quenched. This seems reasonable since the dsDNA assembly of 60 bp can be expected to be standing at the surface nearly with the same angle as the dsDNA assembly of 40 bp.

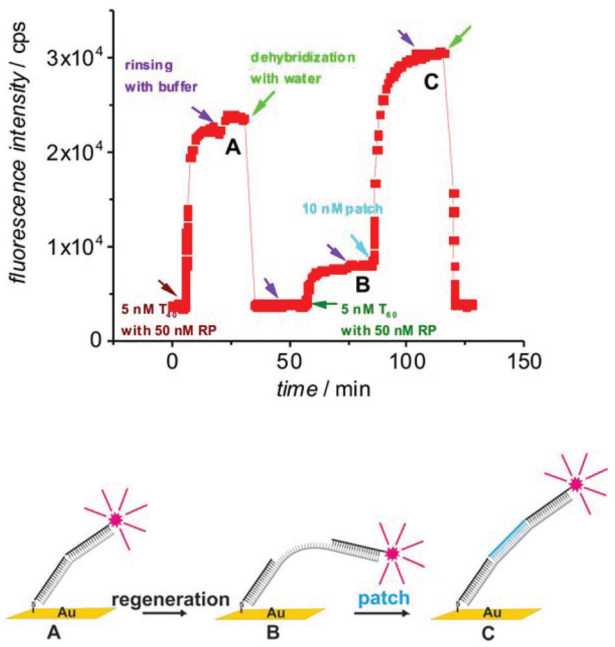

Fig. 3 SPFS kinetic scan curve comparing the fluorescence increase for the detection of the target T_{40} (A) and the target T_{60} before (B) and after incubation with 200 μL of a solution containing the patch at 10 nM (C). The targets were incubated after mixing 100 μL of target solution at a concentration of 10 nM with 100 μL of a solution containing the reporter probe (RP) at 100 nM (final target concentration: 5 nM). After detection of the targets the sensor surface was regenerated by dehybridization with pure water followed by equilibration with buffer.

Reusability of the sensor chip

As is shown in Fig. 2 (see also ESI, Fig. S3–S5†) complete dehybridization of the target by rinsing with pure water was possible and the sensor chips could be used several times without significant fluctuation. By estimating the relative standard deviation (RSD) of the fluorescence increase over three independent detection events as shown in Fig. 2B, values between 0.9% and 4.8% were achieved, depending on the target

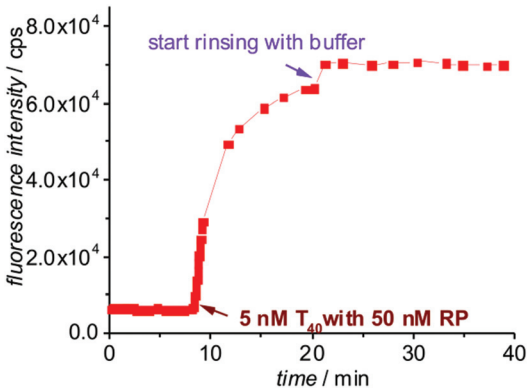

Fig. 4 SPFS kinetic scan curve collected during the detection of the target T_{40} incubated after mixing 100 μL of a target containing solution at a concentration of 10 nM with 100 μL of a 100 nM solution (final target concentration: 5 nM) and subsequent rinsing with buffer solution at a flow rate of 3 mL min^{-1}.

Open Access Article. Published on 25 July 2016. Downloaded on 10/25/2025 11:51:01 PM.
This article is licensed under a Creative Commons Attribution-NonCommercial 3.0 Unported Licence.

concentration (0 nM, 0.9%; 0.05 nM, 1.6%; 0.5 nM, 2.5%; 5 nM, 4.8%; 50 nM, 2.3%). The high stability of the capture probe layer during multiple hybridization/dehybridization steps might be attributed to the three dithiane rings used for chemisorption of the capture probe.[57,58] Also the mild dehybridization procedure by rinsing with pure water may help to conserve the sensor surface.[44,59] When in contrast to rinsing with pure water the sensor chips were rinsed with buffer solution after hybridization with the target, after a few minutes the fluorescence signal became constant. A corresponding experiment for the detection of the target $\mathbf{T_{40}}$ is shown in Fig. 4.

Conclusions

A new sandwich-like strategy has been developed to detect oligonucleotide targets of variable lengths after hybridization to a surface grafted capture probe by SPFS. Even though the targets are hybridized also to a reporter probe, the detection strategy can be termed label-free, since individual targets can be detected directly without previous chemical modification. Following the new detection strategy the background fluorescence could be significantly lowered in comparison with the use of ordinary surface grafted molecular beacons. As a result the detection limit could be decreased by at least one order of magnitude down to a concentration of 50 pM. This detection limit was reached for the forty bases containing target $\mathbf{T_{40}}$ and for the sixty bases containing target $\mathbf{T_{60}}$ (for the latter target the detection procedure included patching). The fact that a similar detection limit can be reached for both targets seems reasonable, since the fluorescence intensity for the detection of $\mathbf{T_{60}}$ at a fixed concentration is only about 20% higher than that of $\mathbf{T_{40}}$ (as shown in Fig. 3). The detection limit did not depend on the sequence of the detection procedure, *i.e.* whether the target and reporter probe were hybridized prior to incubation or the hybridization steps were carried out stepwise. In the current study we did not investigate the influence of single base mismatches, and a possible disadvantage during the detection of long targets might be that with increasing target length, *i.e.* with an increasing number of bases, the influence of a single base mismatch will become less pronounced. Here the sandwich-like detection strategy offers plenty of possibilities for tailor-made solutions. If for instance the mismatch has to be discriminated at the bases close to one of the ends of the target sequence, either the length of the capture probe or the length of the reporter probe can be chosen rather short in order to enlarge the influence of a single base mismatch on the hybridization event at that part. If the mismatch is expected at the center region of a longer target, longer sequences for capture and reporter probes could be applied in combination with a rather short and thus sensitive patch, which is used to trace the mismatch. To further increase the sensitivity against single base mismatches, locked nucleic acid (LNA) or peptide nucleic acid (PNA) could be applied instead of DNA, since for these DNA analogues less base pairs are sufficient for strong hybridization at room temperature. As a consequence the influence of one mismatch will be more pronounced. By the use of LNA or PNA instead of DNA, the detection of relatively short targets such as micro-RNA also becomes possible following the sandwich-like detection strategy. Based on the sandwich-like detection strategy a modular construction system becomes available, which can be applied for the label-free detection of any type of oligonucleotide. The detection of a single target takes only a few minutes, and the sensor chips can be reused many times. With respect to the detection limit it is worth noting that we give the corresponding value in the unit of a concentration. Due to the employed flow cell a total volume of 200 μL was injected for about 15 min leading to a detection limit of 50 pM. As the volume of the applied flow cell is around 100 μL there is a rather large distance between the surface and the opposite cell wall, and thus we are working at semi-infinite diffusion instead of binding all molecules present in the sample. Due to the fact that in principle fluorescence measurements allow the detection down to the single molecule level,[60] it should be possible to significantly lower the detection limit (defined as a concentration or alternatively as an absolute number of molecules bound to a certain surface area) already by improvements of the experimental setup (*e.g.* by microfluidics using a thinner flow cell with smaller volume).

Acknowledgements

We thank David Stephan for experimental support. This work has received funding from the European Research Council under the European Community's Seventh Framework Programme (FP7/2007–2013)/ERC Grant agreement no 240544, from the country North Rhine-Westphalia, and the University of Siegen.

References

1 A. Abi and E. E. Ferapontova, *Anal. Bioanal. Chem.*, 2013, **405**, 3693–3703.
2 A. A. Lubin and K. W. Plaxco, *Acc. Chem. Res.*, 2010, **43**, 496–505.
3 R. P. Johnson, J. A. Richardson, T. Brown and P. N. Bartlett, *J. Am. Chem. Soc.*, 2012, **134**, 14099–14107.
4 J. Dostálek and W. Knoll, *Biointerphases*, 2008, **3**, FD12–FD22.
5 F. Xia, R. J. White, X. Zuo, A. Patterson, Y. Xiao, D. Kang, X. Gong, K. W. Plaxco and A. J. Heeger, *J. Am. Chem. Soc.*, 2010, **132**, 14346–14348.
6 E. Papadopoulou, N. Gale, J. Thompson, T. Fleming, T. Brown and P. Bartlett, *Chem. Sci.*, 2016, **7**, 386–393.
7 S. Mahajan, J. Richardson, T. Brown and P. N. Bartlett, *J. Am. Chem. Soc.*, 2008, **130**, 15589–15601.
8 K. Tawa and W. Knoll, *Nucleic Acids Res.*, 2004, **32**, 2372–2377.
9 D. J. Caruana and A. Heller, *J. Am. Chem. Soc.*, 1999, **121**, 769–774.

 This journal is © The Royal Society of Chemistry 2016

Open Access Article. Published on 25 July 2016. Downloaded on 10/25/2025 11:51:01 PM.
This article is licensed under a Creative Commons Attribution-NonCommercial 3.0 Unported Licence.

10 Y. C. Cao, R. Jin and C. A. Mirkin, *Science*, 2002, **297**, 1536–1540.
11 C.-Y. Zhang, H.-C. Yeh, M. T. Kuroki and T.-H. Wang, *Nat. Mater.*, 2005, **4**, 826–831.
12 B. S. Gaylord, A. J. Heeger and G. C. Bazan, *J. Am. Chem. Soc.*, 2003, **125**, 896–900.
13 P. M. Holland, R. D. Abramson, R. Watson and D. H. Gelfand, *Proc. Natl. Acad. Sci. U. S. A.*, 1991, **88**, 7276–7280.
14 W. H. Koch, *Nat. Rev. Drug Discovery*, 2004, **3**, 749–761.
15 D. Whitcombe, J. Theaker, S. P. Guy, T. Brown and S. Little, *Nat. Biotechnol.*, 1999, **17**, 804–807.
16 N. E. Broude, *Trends Biotechnol.*, 2002, **20**, 249–256.
17 B. Dubertret, M. Calame and A. J. Libchaber, *Nat. Biotechnol.*, 2001, **19**, 365–370.
18 S. Tyagi, D. P. Bratu and F. R. Kramer, *Nat. Biotechnol.*, 1998, **16**, 49–58.
19 S. Tyagi and F. R. Kramer, *Nat. Biotechnol.*, 1996, **14**, 303–308.
20 X. Fang, X. Liu, S. Schuster and W. Tan, *J. Am. Chem. Soc.*, 1999, **121**, 2921–2922.
21 G. Yao and W. Tan, *Anal. Biochem.*, 2004, **331**, 216–223.
22 H. Wang, J. Li, H. Liu, Q. Liu, Q. Mei, Y. Wang, J. Zhu, N. He and Z. Lu, *Nucleic Acids Res.*, 2002, **30**, e61/61–e61/69.
23 H. Du, M. D. Disney, B. L. Miller and T. D. Krauss, *J. Am. Chem. Soc.*, 2003, **125**, 4012–4013.
24 G. Yao, X. Fang, H. Yokota, T. Yanagida and W. Tan, *Chem. – Eur. J.*, 2003, **9**, 5686–5692.
25 J. Wang, D. Onoshima, M. Aki, Y. Okamoto, N. Kaji, M. Tokeshi and Y. Baba, *Anal. Chem.*, 2011, **83**, 3528–3532.
26 H. Du, C. M. Strohsahl, J. Camera, B. L. Miller and T. D. Krauss, *J. Am. Chem. Soc.*, 2005, **127**, 7932–7940.
27 C. M. Strohsahl, H. Du, B. L. Miller and T. D. Krauss, *Talanta*, 2005, **67**, 479–485.
28 C. M. Strohsahl, T. D. Krauss and B. L. Miller, *Biosens. Bioelectron.*, 2007, **23**, 233–240.
29 H.-I. Peng, C. M. Strohsahl, K. E. Leach, T. D. Krauss and B. L. Miller, *ACS Nano*, 2009, **3**, 2265–2273.
30 C. M. Strohsahl, B. L. Miller and T. D. Krauss, *Nat. Protoc.*, 2007, **2**, 2105–2110.
31 H.-I. Peng, T. D. Krauss and B. L. Miller, *Anal. Chem.*, 2010, **82**, 8664–8670.
32 S.-H. Cao, T.-T. Xie, W.-P. Cai, Q. Liu and Y.-Q. Li, *J. Am. Chem. Soc.*, 2011, **133**, 1787–1789.
33 J. R. Lakowicz, *Anal. Biochem.*, 2004, **324**, 153–169.
34 A. A. Lubin, R. Y. Lai, B. R. Baker, A. J. Heeger and K. W. Plaxco, *Anal. Chem.*, 2006, **78**, 5671–5677.
35 Y. Xiao, R. Y. Lai and K. W. Plaxco, *Nat. Protoc.*, 2007, **2**, 2875–2880.
36 K. J. Cash, A. J. Heeger, K. W. Plaxco and Y. Xiao, *Anal. Chem.*, 2009, **81**, 656–661.
37 Y. Xiao, X. Lou, T. Uzawa, K. J. I. Plakos, K. W. Plaxco and H. T. Soh, *J. Am. Chem. Soc.*, 2009, **131**, 15311–15316.
38 D. Kang, A. Vallee-Belisle, A. Porchetta, K. W. Plaxco and F. Ricci, *Angew. Chem., Int. Ed.*, 2012, **51**, 6717–6721.
39 A. J. Simon, A. Vallee-Belisle, F. Ricci, H. M. Watkins and K. W. Plaxco, *Angew. Chem., Int. Ed.*, 2014, **53**, 9471–9475.
40 A. Idili, A. Amodio, M. Vidonis, J. Feinberg-Somerson, M. Castronovo and F. Ricci, *Anal. Chem.*, 2014, **86**, 9013–9019.
41 T. Neumann, M. L. Johansson, D. Kambhampati and W. Knoll, *Adv. Funct. Mater.*, 2002, **12**, 575–586.
42 T. Liebermann, W. Knoll, P. Sluka and R. Herrmann, *Colloids Surf., A*, 2000, **169**, 337–350.
43 L. Touahir, A. T. A. Jenkins, R. Boukherroub, A. C. Gouget-Laemmel, J.-N. Chazalviel, J. Peretti, F. Ozanam and S. Szunerits, *J. Phys. Chem. C*, 2010, **114**, 22582–22589.
44 Q. Su, D. Wesner, H. Schönherr and G. Nöll, *Langmuir*, 2014, **30**, 14360–14367.
45 Y. V. Gerasimova and D. M. Kolpashchikov, *Chem. Soc. Rev.*, 2014, **43**, 6405–6438.
46 J. Kim and M.-Y. Yoon, *Analyst*, 2010, **135**, 1182–1190.
47 M. Ranki, A. Palva, M. Virtanen, M. Laaksonen and H. Söderlund, *Gene*, 1983, **21**, 77–85.
48 Z. Gryczynski, I. Gryczynski, E. Matveeva and J. Borejdo, *US Pat*, 20090218516A1, 2012.
49 G. Nöll, Q. Su, B. Heidel and Y. Yu, *Adv. Healthcare Mater.*, 2014, **3**, 42–46.
50 Y. Yu, B. Heidel, T. L. Parapugna, S. Wenderhold-Reeb, B. Song, H. Schönherr, M. Grininger and G. Nöll, *Angew. Chem., Int. Ed.*, 2013, **52**, 4950–4953.
51 E. L. S. Wong, E. Chow and J. J. Gooding, *Langmuir*, 2005, **21**, 6957–6965.
52 S. Vogt, Q. Su, C. Gutiérrez-Sánchez and G. Nöll, *Anal. Chem.*, 2016, **88**, 4383–4390.
53 A. Samoc, A. Miniewicz, M. Samoc and J. G. Grote, *J. Appl. Polym. Sci.*, 2007, **105**, 236–245.
54 J. A. De Feijter, J. Benjamins and F. A. Veer, *Biopolymers*, 1978, **17**, 1759–1772.
55 L. Lee, A. P. R. Johnston and F. Caruso, *Biomacromolecules*, 2008, **9**, 3070–3078.
56 A. W. Peterson, R. J. Heaton and R. M. Georgiadis, *Nucleic Acids Res.*, 2001, **29**, 5163–5168.
57 P. Liepold, T. Kratzmüller, N. Persike, M. Bandilla, M. Hinz, H. Wieder, H. Hillebrandt, E. Ferrer and G. Hartwich, *Anal. Bioanal. Chem.*, 2008, **391**, 1759–1772.
58 J.-S. Lee, A. K. Lytton-Jean, S. J. Hurst and C. A. Mirkin, *Nano Lett.*, 2007, **7**, 2112–2115.
59 N. Phares, R. J. White and K. W. Plaxco, *Anal. Chem.*, 2009, **81**, 1095–1100.
60 J. R. Lakowicz, K. Ray, M. Chowdhury, H. Szmacinski, Y. Fu, J. Zhang and K. Nowaczyk, *Analyst*, 2008, **133**, 1308–1346.